ISSN 1330-3651 (Print), ISSN 1848-6339 (Online)
DOI: 10.17559/TV-20150314105216

# INFLUENCING FACTOR ANALYSIS AND DISPLACEMENT PREDICTION IN RESERVOIR LANDSLIDES − A CASE STUDY OF THREE GORGES RESERVOIR (CHINA)

*Faming Huang, Kunlong Yin, Tao He, Chao Zhou, Jun Zhang*

Subject review

The developmental tendencies of cumulative displacement time series associated with reservoir landslides influenced by large water reservoirs must be effectively predicted. However, traditional methods do not encompass the dynamic response relationships between landslide deformation and its influencing factors. Therefore, a new approach based on the exponential smoothing (ES) and multivariate extreme learning machine methods was introduced to reveal the influencing factors of landslide deformation and to forecast landslide displacement values. First, the influencing factors of reservoir landslide deformation were analysed. Second, the ES method was used to predict the trend term displacement and obtain the periodic term displacement by determining the trend term from the cumulative displacement. Next, multivariate influencing factors were analysed to explain the periodic term displacement. Then, an extreme learning machine (ELM) model was established to predict the periodic term displacement based on the multivariable analysis of influencing factors. Finally, cumulative displacement prediction values were obtained by adding the trend and periodic displacement prediction values. The Bazimen and Baishuihe landslides in Three Gorges Reservoir Area (TGRA) were selected as case studies. The proposed ES-multivariate ELM (ES-MELM) model was compared to the ES-univariate ELM (ES-ELM) model. The results show that reservoir landslide deformation is mainly influenced by periodic reservoir water level fluctuations and heavy rainfall. Additionally, the proposed model yields more accurate predictions than the ES-ELM model.

***Keywords:*** *displacement prediction; exponential smoothing; Extreme Learning Machine; multivariate influencing factors; reservoir landslide; Three Gorges Reservoir*

**Analiza faktora utjecaja i predviđanje pomaka klizišta akumulacije – studija slučaja Three Gorges Reservoir (Kina)**

Pregledni članak

Potrebno je učinkovito predviđati kako će se vremenski odvijati kumulativni pomaci povezani s klizištima akumulacija. Međutim, tradicionalne metode ne obuhvaćaju dinamički uspostavljene odnose između deformacije klizišta i faktora koji na to utječu. Dakle, uveden je novi pristup na temelju eksponencijalnog izglađivanja (EI) i multivarijatnih metoda ekstremno učećeg stroja kako bi se otkrili čimbenici od utjecaja na deformacije klizišta i predvidjele vrijednosti pomaka klizišta. Prvo su analizirani faktori koji utječu na deformacije klizišta akumulacije. Zatim je EI postupak rabljen za predviđanje trajanja trenda pomaka i dobivanje trajanja periodičnog pomaka određivanjem trajanja trenda iz kumulativnog pomaka. Dalje, analizirani su multivarijatni utjecajni faktori kako bi objasnili trajanje periodičnog pomaka. Nakon toga, postavljen je model ekstremno učećeg stroja kako bi se predvidjelo trajanje periodičnog pomaka na temelju multivarijatne analize utjecajnih čimbenika. Konačno, dobivene su vrijednosti predviđanja kumulativnog pomaka dodavanjem vrijednosti predviđanja trenda i periodičnog pomaka. Bazimen i Baishuihe klizišta u području Three Gorges Reservoir odabrana su kao studije slučaja. Predloženi model EI-multivarijatnog ekstremno učećeg stroja (ES-MELM) uspoređen je s modelom EI-univarijantnog ekstremno učećeg stroja (ES-ELM). Rezultati pokazuju da je deformacija klizišta akumulacije uglavnom pod utjecajem periodičnih oscilacija razine vode akumulacije i obilnih kiša. Osim toga, predloženi model pridonosi točnijem predviđanju od ES-ELM modela.

***Ključne riječi:*** *eksponencijalno izglađivanje (EI); ekstremno učeći stroj (Extreme Learning Machine); klizište akumulacije; predviđanje pomaka; multivarijantni faktori utjecaja; Three Gorges Reservoir*

## 1 Introduction

To meet the needs of flood control and clean energy, many large-scale hydropower projects have been built. Large dams have attracted attention not only for their enormous economic benefits but also because they cause environmental degradation and increasingly frequent geological disasters [1, 2]. For example, Three Gorges Dam in China, which is one of the largest water conservation projects, has led to the reactivation of many reservoir landslides [3, 4]. Reservoir landslides are more likely to be reactivated because of rapid groundwater level fluctuations, which are mainly caused by heavy rainfall and reservoir water level fluctuations [5÷8]. People's lives and property can be seriously threatened by reactivated reservoir landslides. Therefore, future landslide development and deformation must be predicted [9].

Landslide monitoring plays an important role in early warnings of landslide failure. Global Positioning Systems (GPS), rain gauges, groundwater level monitoring equipment and other instruments have been frequently used by geological engineers to monitor reservoir landslides [10, 11]. Additionally, many researchers [12÷14] have focused on the regularity of monitoring data. They suggest that reservoir landslide deformation is continuous under the joint actions of geological conditions and external factors. Thus, monthly cumulative displacement can be decomposed into a trend item and a monthly periodic term. The trend item values reflect future development and the slope potential energy under the control of geological conditions, such as the landslide terrain structure, the permeability coefficient, and the shear strength. The monthly periodic term values reflect periodic characteristics, which are influenced by external factors such as the reservoir water level and seasonal rainfall. The exponential smoothing (ES) method [15, 16], which predicts test data using historical data through stepwise regression, is used to predict the trend item values of cumulative displacement. Meanwhile, the cumulative displacement was decomposed into trend item and monthly periodic term values by subtracting the trend item values from the cumulative displacement values.

Some displacement prediction models that use decomposition have been proposed based on the influence of rainfall and the reservoir water level on monthly periodic displacement [17, 18]. This study will also explore the relationship between the monthly periodic term displacement and external factors [19÷22] to advance model construction. Multivariate prediction models, which contain abundant information about complex non-linear

systems, will be used to predict monthly periodic item values if landslide displacement is dependent on influencing factors [23÷25]. Following multivariate dependence analyses, mathematical models such as the local linear model [26÷28], artificial neural network (ANN)[29÷31], Volterra adaptive model [32, 33], support vector machine (SVM) [34, 38], Extreme Learning Machine [39÷41] and others have been used for multivariate time series prediction. Among these mathematical models, ELM exhibits many unique advantages in solving small sample size, nonlinear and high-dimensional pattern recognition problems. Therefore, ELM [42] is used to predict the monthly periodic term displacement in this study.

As discussed above, the trend term values of cumulative displacement will be predicted using the ES method. The monthly periodic term values of cumulative displacement will be predicted by a multivariable ELM model. The final predicted values can be obtained by adding the predicted trend term values and periodic term values. A hybrid model based on the ES method and multivariate ELM (ES-MELM model) is proposed to discuss the effects of influencing factors on landslide deformation and to predict the cumulative landslide displacement values. Baishuihe landslide and Bazimen landslide (Fig. 1) in the TGRA are taken as examples. The ES-ELM model based on the ES method and uni-variable ELM without considering influencing factors was used for comparison.

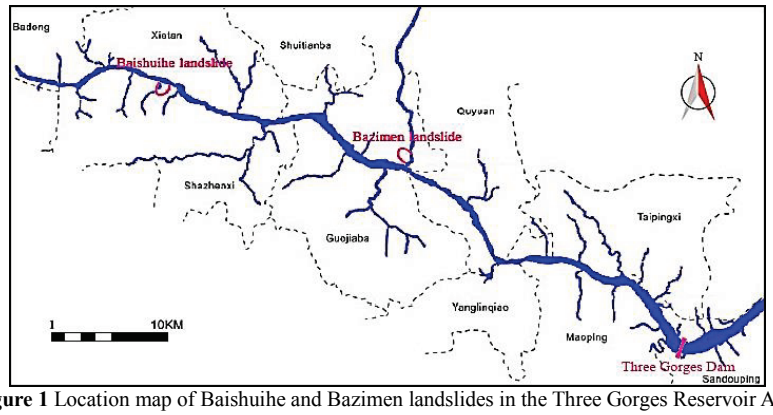


**Figure 1** Location map of Baishuihe and Bazimen landslides in the Three Gorges Reservoir Area

## 2 Methodologies

The ES-MELM model includes four steps. First, the dependence of cumulative displacement on monthly rainfall and monthly average reservoir water level were analysed. Second, trend displacement was predicted using the ES method. Third, the influencing factors were used to analyse and predict monthly periodic term displacement using the ELM model. Finally, the total displacement prediction value was obtained by adding the trend and monthly periodic prediction values. A flowchart of the proposed model is shown in Fig. 2.

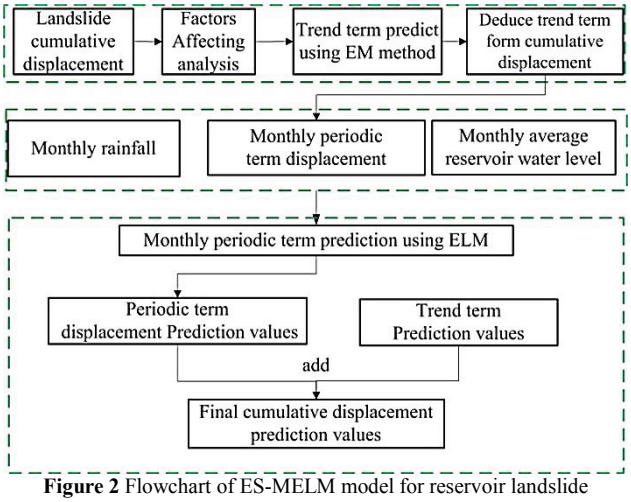


**Figure 2** Flowchart of ES-MELM model for reservoir landslide displacement prediction

### 2.1 Exponential smoothing

The ES [14] method is excellent for real-time forecast. It weights the observed time series unequally by time. Recent observations are weighted more heavily than older observations. In this paper, double exponential smoothing (DES) was used to forecast the basic trend characteristics of landslide displacement time series. Assuming that $y_1, y_2, \cdots, y_t$ represent a displacement time series, the single exponential smoothing formula is as follows:

$$S_t' = \alpha Y_{t-1} + (1-\alpha) S_{t-1}' \quad (1)$$

Suppose that the single exponential smoothing value of the first t times is $S_t'$, then the prediction formula DES value $S_t''$ of the first t times is as follows:

$$S_t'' = \alpha S_{t-1}' + (1-\alpha) S_{t-1}'' \quad (2)$$

In Eqs. (1) and (2), $S_{t-1}'$ and $S_{t-1}''$ are single and double exponential smoothing values of the first $t-1$ times, respectively. $Y(t)$ is the actual monitoring value for the first $t$ landslide displacement. The parameter $\alpha \in [0, 1)$ determines the degree of exponential decay.

### 2.2 Principle of Extreme Learning Machine

Extreme Learning Machine [43] is a single-hidden layer feed forward neural network (SLFN) with randomly generated hidden nodes that are independent of the training data. Input weights and biases can be randomly chosen, and output weights can be analytically determined using the

Moore-Penrose (MP) generalized inverse. Compared with traditional popular gradient-based learning algorithms for SLFNs, ELM not only learns much faster with higher generalization ability but also avoids many difficulties associated with stopping criteria, learning rates, learning epochs, and local minima. The ELM model has been used in many areas, such as time series prediction [44, 45], image quality assessment [46], classification [47, 48], face recognition [49, 50] and others. The structure of ELM is illustrated in Fig. 3.

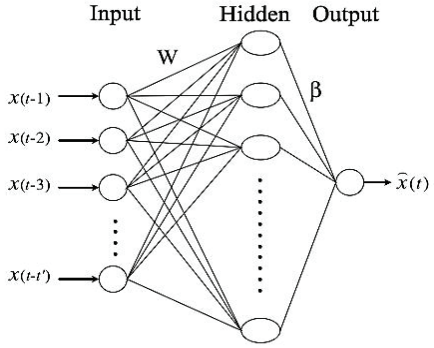


**Figure 3** Structure of ELM model

For $N$ distinct samples $(x_i, t_i)$, where $x_i = [x_{i1}, x_{i2}, \ldots, x_{in}]T \in R_n$ and $t_i = [t_{i1}, t_{i2}, \ldots, t_{im}]T \in R_m$, standard SLFNs with $\tilde{N}$ hidden neurons and activation function $g(x)$ are mathematically modelled as follows.

$$\sum_{i=1}^{\tilde{N}} \beta_i g(w_i x_j + b_i) = o_j, j = 1, 2, \cdots, N. \quad (6)$$

where $w_i = [w_{i1}, w_{i2}, \ldots, w_{in}]^T$ is the weight vector of the connections between the input neurons and the $i^{th}$ hidden neuron, $\beta_i = [\beta_{i1}, \beta_{i2}, \ldots, \beta_{im}]^T$ is the weight vector connecting the $i$th hidden neuron and the output neuron,; $o_i = [o_{j1}, o_{j2}, \ldots, o_{jm}]^T$ is the $j^{th}$ output vector of the SLFN and $b_i$ is the threshold of the $i^{th}$ hidden neuron. $w_i \cdot x_j$ denotes the inner product of $w_i$ and $x_j$. The above $N$ equations can be written compactly as follows:

$$H\beta = O \quad (7)$$

where

$$\begin{bmatrix} g(w_1 x_1 + b_1) & \cdots & g(w_{\tilde{N}} x_1 + b_{\tilde{N}}) \\ \vdots & \ddots & \vdots \\ g(w_1 x_N + b_1) & \cdots & g(w_{\tilde{N}} x_N + b_{\tilde{N}}) \end{bmatrix}_{N \times \tilde{N}}$$

$$\beta = \begin{bmatrix} \beta_1^T \\ \vdots \\ \beta_{\tilde{N}}^T \end{bmatrix}_{\tilde{N} \times m} \text{ and } O = \begin{bmatrix} o_1^T \\ \vdots \\ o_{\tilde{N}}^T \end{bmatrix}_{N \times m} \quad (8)$$

$H$ is the hidden-layer output matrix of the neural network. The $i^{th}$ column of $H$ is the $i^{th}$ hidden neuron's output vector with respect to inputs $x_1, x_2, \ldots, x_N$.

ELM theories claim that the input weights $w_i$ and hidden biased $b_i$ can be randomly generated instead of tuned. To minimize the cost function $\| O-T \|$, where $T = [t_1, t_2, \ldots, t_N]^T$ is the target value matrix, the output weights are based on the least-square (LS) solution to the linear system $H\beta=T$:

$$X_{\text{normalize}} = \frac{(x_{ij} - \max\{x_{ij}\}) + (x_{ij} - \min\{x_{ij}\})}{(\max\{x_{ij}\} - \min\{x_{ij}\})}, \quad (9)$$
$$i = 1, 2, \cdots, N;\ j = 1, 2, \cdots, N.$$

The un-normalized method for the input and output data set is as follows:

$$O_{\text{normalize}} = \frac{o_{ij}(\max\{x_{ij}\} - \min\{x_{ij}\}) + (\max\{x_{ij}\} + \min\{x_{ij}\})}{2} \quad (10)$$
$$i = 1, 2, \cdots, N;\ j = 1, 2, \cdots, N.$$

The hidden notes considerably influence the predictive ability of ELM. In this study, the number of hidden notes was set as a small default value (15) for all prediction models.

## 3 Case studies

The TGRA [51, 52] is located at the junction of the Yangtze River Basin and Sichuan Basin, encompassing a total area of 5,67×104 km$^2$ and covering a total mainstream segment length of 574 km. The construction of Three Gorges Dam began in 1994. The dam began to store water in 2003. We have surveyed 5386 landslides in the TGRA since December 2009. Two reservoir landslides in the TGRA, Baishuihe landslide and Bazimen landslide, were selected as case studies to analyse influencing factors and displacement prediction.

### 3.1 Baishuihe landslide

#### 3.1.1 Geological conditions

Baishuihe landslide [53, 54], which lies on the southern Yangtze River, is located in Shazhenxi in Zigui county. The bedrock ridges located to the east and west are considered landslide boundaries. The elevation of the landslide ranges from 70 m to 300 m, and the length from the north to south is 780 m, while the width from the east to the west is 700 m$^3$. A topographical map depicting the monitoring network is shown in Fig. 4.

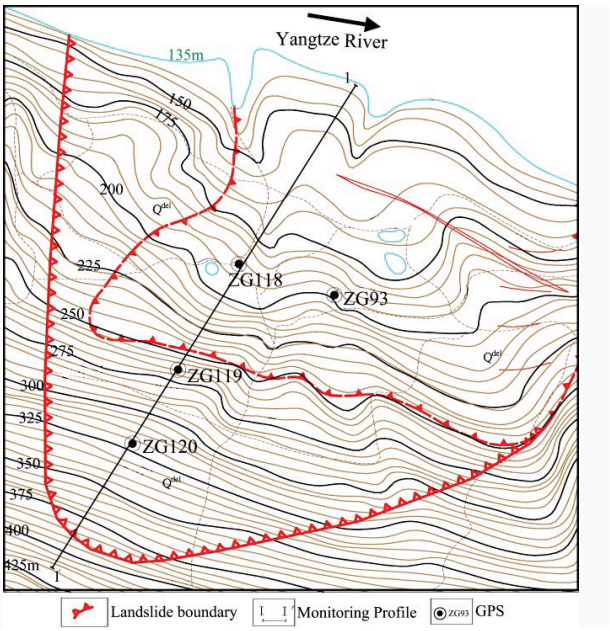


**Figure 4** Topographical map of Baishuihe landslide, with the location of GPS monitoring stations

This landslide is mainly composed of quaternary residual deposits and accumulations. The formation lithology comprises thick, bedded Jurassic sandstone and thin. The main development direction of joint fissures is nearly east-west, with north-south dipping fractures. Schematic crosssection I-I' is shown in Fig. 5.

Clear macroscopic signs of deformation have appeared on the surface of Baishuihe landslide since June 2003. Six GPS monitoring stations and other professorial monitoring devices were arranged to monitor landslide deformation from November 2003 to January 2009. The landslide displacement system used in this study contained ZG118 GPS monitoring displacement time series $R_{1i}$ ($i$ = 1, 2, …, 63)in a strong deformation area, monthly rainfall time series $S_{1i}$ ($i$ = 1, 2, …, 63), and monthly average water level series $T_{1i}$ ($i$ = 1, 2, …, 63). For the Baishuihe landslide displacement system, the first 48 displacement time series from November 2003 to October 2007 were used for model training, and the 15 displacement time series from November 2007 to January 2009 were used to test the model.

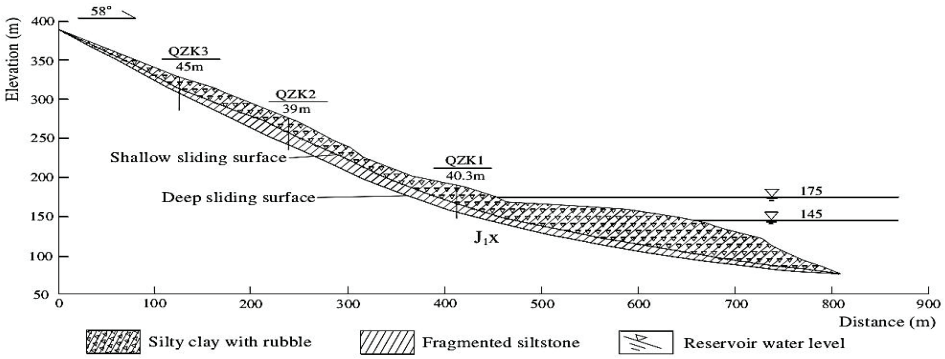


**Figure 5** Geological section I-I'of Baishuihe landslide

### 3.1.2 Analysis of influencing factors

Before displacement prediction using the EM-MELM model, it is necessary to analyse the dependence of cumulative displacement on its influencing factors. The Baishuihe landslide displacement system is shown in Fig. 6. It can be observed that the ZG118 cumulative displacement curve shows step-style evolution characteristics under the influence of the seasonal rainfall and periodic fluctuations of the reservoir level.

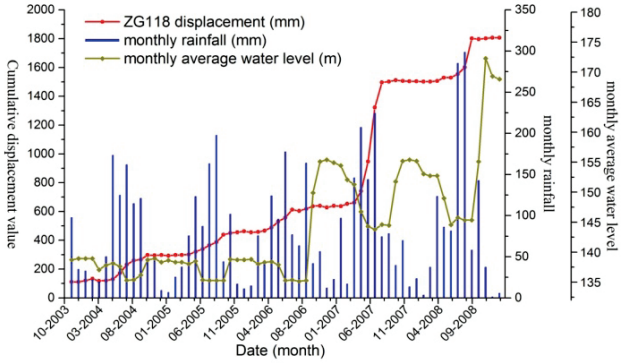


**Figure 6** Correlation curve of rainfall, water level and displacement on Baishuihe landslide

Severe deformation can be observed during the rainy season, and there is little deformation in the dry season. As is shown from April to August 2007, monthly rainfall increases drastically, and landslide displacement rapidly increased from 600 mm to 1450 mm in this period. Smaller rainfall amounts from January to March 2008 were associated with almost no deformation. Another example extends from May to August 2004 in the rainy season, when there was severe landslide deformation. However, deformation became less severe during the winter. Meanwhile, little landslide deformation occurred when the water level was high and stable. It can be observed that landslide deformation was not severe from November 2006 to April 2007 when the water level remained at 155 m, but when the water level declined from 175 m to 140 m, landslide deformation increased significantly. When the water level fluctuated cyclically from 145÷175 m, landslide deformation displayed a similar trend. These phenomena indicate that water level fluctuations and seasonal rainfall had significant impacts on Baishuihe landslide deformation.

### 3.1.3 Trend item displacement prediction

The DES method (smoothness index=0,8) was used to predict trend item displacement $r_{1i}$ ($i$ = 1, 2, …, 63) and obtain the monthly periodic displacement time series $R'_{1i}$ ($i$ = 1, 2, …, 63), $R_{1i} = R'_{1i} + r_{1i}$. The decomposition results are shown in Fig. 7.

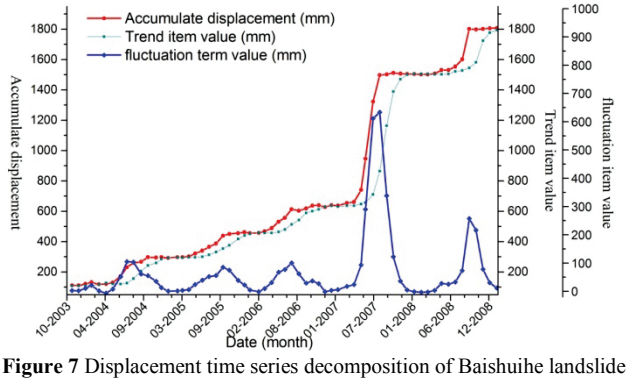


**Figure 7** Displacement time series decomposition of Baishuihe landslide

The monthly periodic displacement time series $R'_{1i}$ and its influencing factors are shown in Fig. 8. Displacement values become alternately large or small due to the combined effects of heavy rainfall and cyclical fluctuations of the water level. Therefore, a multivariate time series based predictor can be used to predict periodic item displacement values.

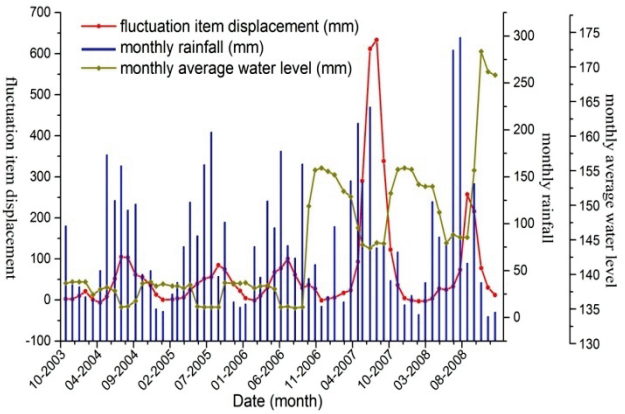


**Figure 8** Correlation curve of monthly periodic term displacement, rainfall and reservoir water level

### 3.1.4 Monthly periodic item prediction using MELM

It is important to select appropriate input variables and output variables for multivariable ELM modelling. The required input variables include monthly rainfall, the monthly reservoir water level and the number of displacements at different time intervals that have a significant influence on the predicted monthly periodic item displacements. The periodic item displacement variation belongs to a multivariate time series. Therefore, in this study, the correlation analysis technique was employed to calculate the input variables from multivariate displacement [55÷57]. As shown in Figure 8, monthly rainfall in the first month ($T_{1,i-1}$), water level fluctuations in the first month ($S_{1,i-1}$), and periodic item displacement in the first two months ($R'_{1,i-2}, R'_{1,i-1}$) strongly influence the displacement and the prediction in the next month $R'_{1,n}$.

Therefore, the multivariate time series used for monthly periodic item predictions are as follows: periodic item displacement time series $R'_{1i}$, monthly average water level $S_{1,i}$, and monthly rainfall $T_{1,i}$ ($i$ = 1, 2, …, 63). The input variables for the MELM model are shown in Eq.(11).

$$V_{i-1} = (R'_{1,i-2}, R'_{1,i-1}, S_{1,i-1}, T_{1,i-1}) \quad (11)$$

where $i$ = 3, 4, …, 63. If the deterministic function $F(V_{i-1})$ is known, $R'_{1,i}$ can be predicted.

$$R'_{1,i} = F(V_{i-1}) \quad (12)$$

The MELM model was used to calculate the deterministic function $F(V_{i-1})$. $V_{i-1}$ was set as the model input variables. $R'_{1,i}$ was set as the model output variables. The final predicted values can be obtained by adding the trend displacement values and monthly periodic displacement values:

$$R_{1,I} = R'_{1,I} + r_{1,i}. \quad (13)$$

In addition, for the ES-ELM model, the input variables were$(R'_{1,i-2}, R'_{1,i-1})$. The output variable was $R'_{1,i}$. The predicted values of monthly periodic item displacement are shown in Fig. 9.

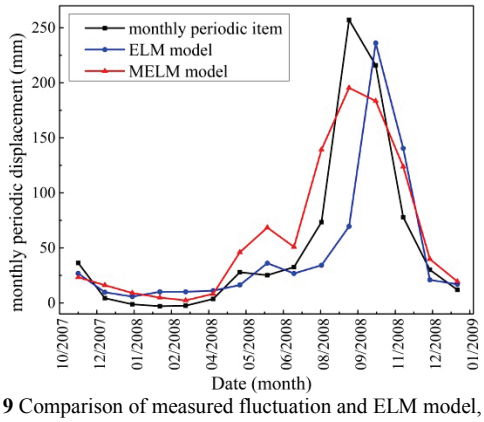


**Figure 9** Comparison of measured fluctuation and ELM model, MELM model

### 3.1.5 Final prediction results using ES-MELM

The final prediction results of cumulative displacement were obtained by adding the trend values predicted using the DES method and the periodic values predicted using the MELM model. The results are shown in Fig. 10 and Tab. 1.

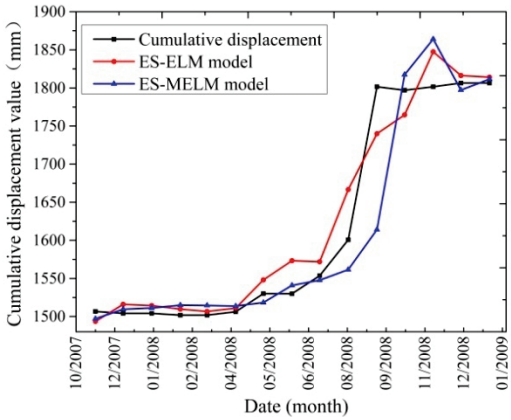


**Figure 10** Comparison of final predicted and measured cumulative displacement values on Baishuihe landslide

In Fig. 10, the ES-ELM model can only predict the basic trend characteristics of landslide displacement, while the EM-MELM model can predict the step-style variational characteristics of the landslide displacement curves. In this study, root-mean-square error (RMSE) and mean absolute percentage error (MAPE) were used as accuracy assessment tools, as shown in Tab. 1. The results in Fig. 10 and Tab. 1 suggest that the prediction accuracy of ES-MELM is higher than that of ES-ELM.

**Table 1**Prediction accuracy comparison between ES-MELM and ES-ELM model

| Model | RMSE / mm | MAPE / % |
|---|---|---|
| ES-MELM | 31,13 | 1,33 |
| ES-ELM | 52,93 | 1,58 |

## 3.2 Bazimen landslide

### 3.2.1 Geological conditions

Bazimen landslide [58, 59] is located on the right bank of the Xiangxi River, which is a major tributary of the Yangtze River. It is a three-level accumulation platform with a grooved shape and main sliding direction of approximately 110° NE. The landslide length is 550 m,

with 350 m located underwater. The landslide width is approximately 80÷120 m. The average thickness of the slip body is approximately 30 m. A topographical map depicting the monitoring network is shown in Fig. 11.

Bazimen landslide is composed of loose Colluvial products and slope sediments. The rock and soil layers are mainly distributed at the centre of the landslide, including a fragmented, silty clay layer, a silty clay offshoot of the fragmented stone layer, and gravel soil layers. The landslide is mainly sliding along the bedrock surface. Colluvial deposits can be observed in the deeper portions of local gullies. A bedrock slide above 139 m level is mainly composed of Lower Jurassic Xiangxi group (J1) layers. Underwater, the Yanchang formation mainly comprises the middle strata (T2). A surface gully has developed in the landslide area. The groundwater aquifer in the study area can be divided into a loosely accumulated pore water aquifer rock group and a bedrock fissure water aquifer rock group. Cross section I-I' is shown in Fig. 12.

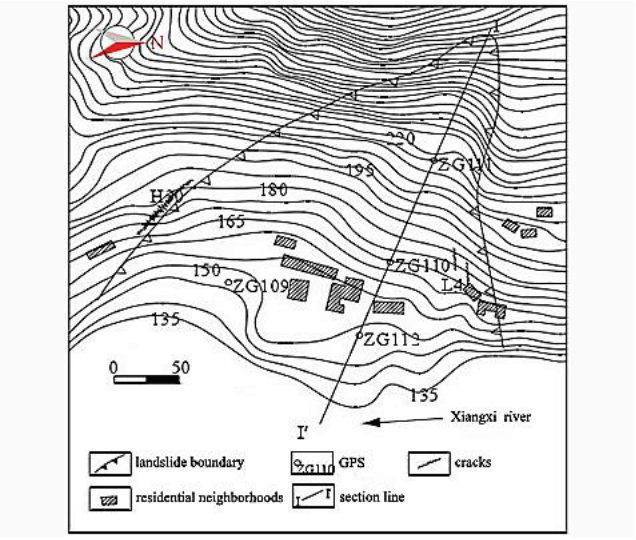


**Figure 11** Topographical map of Bazimen landslide, with the location of GPS monitoring stations

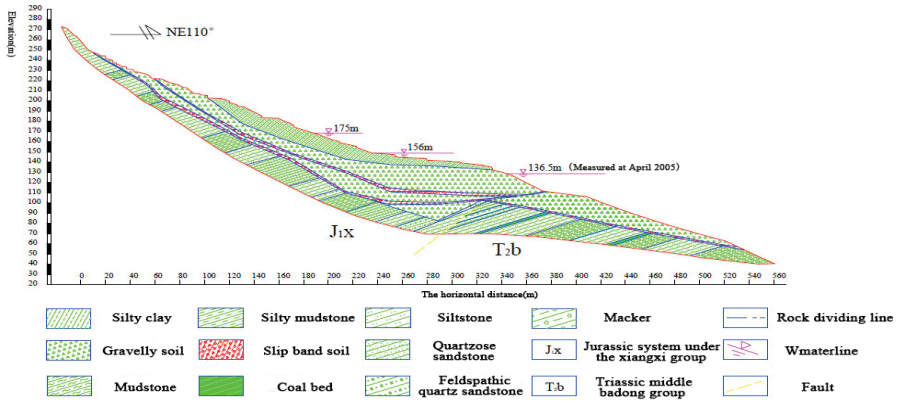


**Figure 12** Geological section I-I' of Bazimen landslide

Four GPS points, rain gauges, and other instruments have been used to monitor landslide deformation since 2003. The ZG111 GPS monitoring displacement time series $R_{2i}$ ($i$ = 1, 2, …, 58), monthly rainfall series $S_{2i}$ ($i$ = 1, 2, …, 58), and monthly average reservoir water level time series $T_{2i}$ ($i$ = 1, 2, …, 58) from August 2003 to October 2008 were selected as case studies. The first 48 time series of the deformation system were used for model training, while the other 10 time series from February 2008 to November 2008 were used for model testing.

### 3.2.2 Analysis of influencing factors

The correlation curves between cumulative displacement, monthly rainfall, and monthly average water level are shown in Fig. 13.

After the impoundment of TGR in June 2003, Bazimen landslide deformed severely. When the water level dropped during the rainy season from May to July 2004, substantial deformation occurred in the middle and upper areas. In June 2005, some existing cracks expanded. Fig. 13 shows that larger rainfall events caused stronger landslide deformation. In addition, when the water level is higher, landslide deformation is less severe, but when the water level falls fast, landslide deformation is more severe. The correlation curves indicate that water level fluctuations and seasonal rainfall are the factors influencing Bazimen landslide deformation.

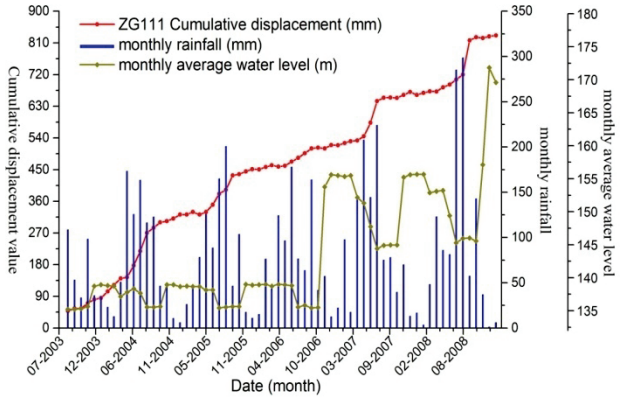


**Figure 13** Correlation curve of cumulative displacement and monthly rainfall, monthly water level

### 3.2.3 Time series decomposition and periodic term predict

The DES method was adopted to predict trend term displacement time series $r_{2,i}$ based on a smoothness index of 0,8. The multivariate time series of the periodic landslide deformation term were as follows: the monthly periodic term displacement time series $R'_{2,i}$, the average monthly water level time series $S_{2,i}$, and the monthly rainfall time series $T_{2,i}$, where $i$ = 1, 2, ..., 58. A correlation analysis was used to calculate the input variables for periodic displacements. The input and output variable analysis of the Bazimen landslide suggested that monthly

rainfall during the first month, water level fluctuations during the first month, and periodic item displacement during the first three months strongly influence the displacement and the prediction in the next month. Multivariate inputs can be reconstructed as follows:

$$V_{i-1} = \left(R'_{2,i-1}, R'_{2,i-2}, R'_{2,i-3}, S_{2,i-1}, T_{2,i-1}\right) \quad (14)$$

where $i = 4, 5, \ldots, 58$. The deterministic function $G(V_n)$ must then be further explored:

$$R'_{2,i} = G(V_{i-1}) \quad (15)$$

The MELM model was used to calculate the deterministic function $G(V_{i-1})$. The input variables were $V_{i-1}$. The output variables were $R'_{2,i}$.

For the ES-ELM model, the input variables were $(R'_{2,i-1}, R'_{2,i-2}, R'_{2,i-3})$, and the output variables were $R'_{2,i}$. Plots of time series decomposition and prediction results for the periodic term displacement are shown in Fig. 14.

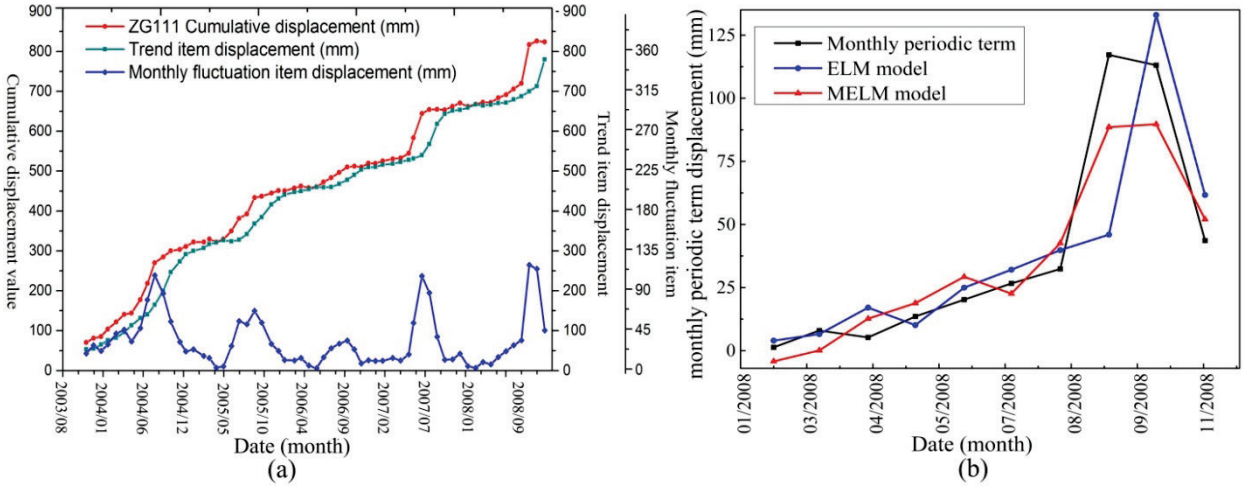


**Figure 14** Time series decomposition of cumulative displacement and periodic term displacement prediction

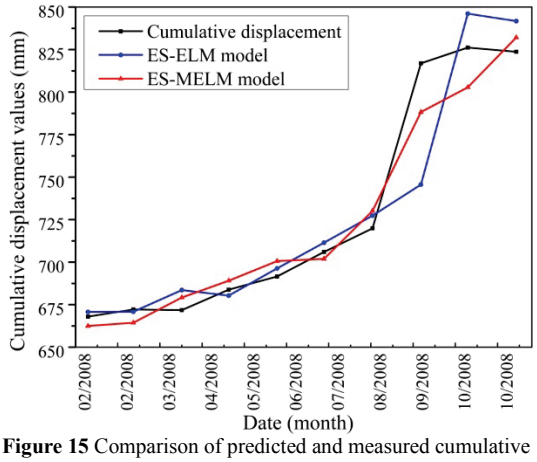


**Figure 15** Comparison of predicted and measured cumulative displacement in Bazimen landslide

### 3.2.4 Final prediction results

The final displacement prediction results are shown in Fig. 15 and Tab. 2. It can be observed that the proposed model produces satisfactory prediction results and exhibits higher prediction accuracy compared to the ES-ELM model.

**Table 2**comparison ofES-MELM and ES-ELM model

| Model | RMSE/ mm | MAPE / % |
|---|---|---|
| ES-MELM | 14,80 | 1,42 |
| ES-ELM | 24,63 | 1,87 |

## 4 Discussion

In this study, the external influencing factors of landslide displacement were analysed. An ES-MELM model based on exponential smoothing and multivariable extreme learning machine methods was proposed to predict landslide displacement values.

For the ES-MELM model, the displacement decomposition results show that the DES method can decompose the cumulative displacement time series into a trend item and periodic item. According to the periodic displacement time series, theBaishuihe and Bazimen landslides exhibit significant relationships between the water level, rainfall, and periodic landslide displacement. The fluctuations of the reservoir water level and heavy rainfall are the main influencing factors of landslide deformation. The water level and rainfall variables must be added to the displacement prediction models to construct a multivariable time series model.

For the ES-ELM and ES-MELM models, the forecast results show that the ES-MELM model displays a higher prediction accuracy compared to the ES-ELM model. The EM-MELM model cannot only efficiently predict the development of cumulative landslide displacement but also reflect the factors that cause landslide deformation. The multivariate time series analysis provides an effective approach for constructing the dynamic response relationship between influencing factors and landslide displacement.

## 5 Conclusions

Reservoir landslides in TGRA are influenced by many factors, and the evolution process of the landslide displacement system exhibits obvious non-linear characteristics. The multivariable time series analysis shows that fluctuations of the reservoir water level and heavy rainfall are the main factors affecting reservoir landslide deformation. The model comparisons show that

the proposed ES-MELM model yields more accurate prediction results than the ES-ELM model with more realistic physical meanings.

**Acknowledgements**

This research was funded by geological disaster risk management of China Geological Survey (NO. 121201122-0173). It was also supported by Science and Technology research projects of Zhejiang Education Department (NO. Y201224800).

## 6 References

[1] Zhang, Q.; Lou, Z. The environmental changes and mitigation actions in the Three Gorges Reservoir region, China. // Environmental Science & Policy. 14, 8(2011), pp. 1132-1138. DOI: 10.1016/j.envsci.2011.07.008

[2] Krzeminska, D. M.; Bogaard, T. A.; Malet, J. P. et al. A model of hydrological and mechanical feedbacks of preferential fissure flow in a slow-moving landslide. // Hydrology & Earth System Sciences. 17, 3(2013), pp. 947-959. DOI: 10.5194/hess-17-947-2013

[3] Fu, B. J.; Wu, B. F.; Lü, Y. H. et al. Three Gorges Project: Efforts and challenges for the environment. // Progress in Physical Geography. 34, 6 (2010), pp. 741-754. DOI: 10.1177/0309133310370286

[4] Wu, S.; Jin, Y.; Zhang, Y. et al. Investigations and assessment of the landslide hazards of Fengdu County in the reservoir region of the Three Gorges project on the Yangtze River. // Environmental Geology. 45, 4(2004), pp. 560-566. DOI: 10.1007/s00254-003-0911-1

[5] Wang, G.; Sassa, K. Pore-pressure generation and movement of rainfall-induced landslides: effects of grain size and fine-particle content. // Engineering geology. 69, 1(2003), pp. 109-125. DOI: 10.1016/S0013-7952(02)00268-5

[6] Priest, G. R.; Schulz, W. H.; Ellis, W. L. et al. Landslide stability: role of rainfall-induced, laterally propagating, pore-pressure waves. // Environmental & Engineering Geoscience. 17, 4(2011), pp. 315-335. DOI: 10.2113/gseegeosci.17.4.315

[7] Can, T.; Nefeslioglu, H. A.; Gokceoglu, C. et al. Susceptibility assessments of shallow earth flows triggered by heavy rainfall at three catchments by logistic regression analyses. // Geomorphology. 72, 1(2005), pp. 250-271. DOI: 10.1016/j.geomorph.2005.05.011

[8] Matsuura, S.; Asano, S.; Okamoto, T. Relationship between rain and/or melt water, pore-water pressure and displacement of a reactivated landslide. // Engineering Geology. 101, 1(2008), pp. 49-59. DOI: 10.1016/j.enggeo.2008.03.007

[9] Eberhardt, E.; Thuro, K.; Luginbuehl, M. Slope instability mechanisms in dipping interbedded conglomerates and weathered marls—the 1999 Rufi landslide, Switzerland. // Engineering Geology. 77, 1 (2005). pp. 35-56. DOI: 10.1016/j.enggeo.2004.08.004

[10] Calcaterra, S.; Cesi, C.; Di Maio, C. et al. Surface displacements of two landslides evaluated by GPS and inclinometer systems: a case study in Southern Apennines, Italy. // Natural hazards. 61, 1(2012), pp. 257-266. DOI: 10.1007/s11069-010-9633-3

[11] Wen, R.; Akbas, B.; Sutchiewchar, N. et al. Inelastic Behaviors of Steel Shear Tab Connections. // The Structural Design of Tall and Special Buildings. 23, 12(2014), pp. 929-946. DOI: 10.1002/tal.1095

[12] Liu, Z.; Shao, J.; Xu, W.; Chen, H.; Shi, C. Comparison on landslide nonlinear displacement analysis and prediction with computational intelligence approaches. // Landslides. 11, 5(2014), pp. 889-896. DOI: 10.1007/s10346-013-0443-z

[13] Jibson, R. W. Regression models for estimating coseismic landslide displacement. // Engineering Geology. 91, 2(2007), pp. 209-218. DOI: 10.1016/j.enggeo.2007.01.013

[14] Corominas, J.; Moya, J.; Ledesma, A.;Lloret, A.;Gili, J. A. Prediction of ground displacements and velocities from groundwater level changes at the Vallcebre landslide (Eastern Pyrenees, Spain). // Landslides. 2, 2(2005), pp. 83-96. DOI: 10.1007/s10346-005-0049-1

[15] Matthys, G.; Beirlant, J. Estimating the extreme value index and high quantiles with exponential regression models. // Statistica Sinica. 13, 3(2003), pp. 853-880.

[16] Hsieh, H. J.; Chen, T.H.; Chang, S. H. Assessing chronic disease progression using non-homogeneous exponential regression Markov models: an illustration using a selective breast cancer screening in Taiwan. // Statistics in Medicine. 21, 22(2002), pp. 3369-3382. DOI: 10.1002/sim.1277

[17] Zeng, Y.; Li C. F. Landslide displacement prediction by using multivariable time series based on RBF neural network. // Journal of Yangtze River Scientific Research Institute. 29, 4(2012), pp. 30-34.

[18] Li, D.; Yin, K. L.; Leo, C. Analysis of Baishuihe landslide influenced by the effects of reservoir water and rainfall. // Environmental Earth Sciences. 60, 4(2010), pp. 677-687. DOI: 10.1007/s12665-009-0206-2

[19] Du, J.; Yin, K. L.; Lacasse, S. Displacement prediction in Colluvial landslides, Three Gorges Reservoir, China. // Landslides. 10, 2(2013), pp. 203-218. DOI: 10.1007/s10346-012-0326-8

[20] Porporato, A.; Ridolfi, L. Multivariate nonlinear prediction of river flows. // Journal of Hydrology. 248, 1(2001), pp. 109-122. DOI: 10.1016/S0022-1694(01)00395-X

[21] Faming, Huang; Kunlong, Yin; Guirong, Zhang et al. Prediction of groundwater level in landslide using multivariable PSO-SVM model. // Journal of Zhejiang University (Engineering Science). 49, 06(2015), pp. 1193-1200.

[22] Dhanya, C. T.; Nagesh Kumar, D. Multivariate nonlinear ensemble prediction of daily chaotic rainfall with climate inputs. // Journal of Hydrology. 403, 3(2011), pp. 292-306. DOI: 10.1016/j.jhydrol.2011.04.009

[23] Rao, A. D.; Sinha, M.; Basu, S. Bay of Bengal wave forecast based on genetic algorithm: A comparison of univariate and multivariate approaches. // Applied Mathematical Modeling. 37, 6(2013), pp. 4232-4244. DOI: 10.1016/j.apm.2012.09.001

[24] Ataei, M.; Lohmann, B.; Khaki-Sedigh, A. et al. Model based method for estimating an attractor dimension from uni/multivariate chaotic time series with application to Bremen climatic dynamics. // Chaos, Solitons & Fractals. 19, 5(2004), pp. 1131-1139. DOI: 10.1016/S0960-0779(03)00300-X

[25] Letellier, C.; Aguirre, L. A. Symbolic observability coefficients for univariate and multivariate analysis. // Physical Review E. 79, 6(2009), pp. 066210. DOI: 10.1103/PhysRevE.79.066210

[26] Vaccari, D. A.; Wang, H. K. Multivariate polynomial regression for identification of chaotic time series. // Mathematical and Computer Modelling of Dynamical Systems. 13, 4(2007), pp. 395-412. DOI: 10.1080/13873950600883691

[27] Chen, Y.; Yang, B.; Dong, J. Time-series prediction using a local linear wavelet neural network. // Neurocomputing, 69, 4(2006), pp. 449-465. DOI: 10.1016/j.neucom.2005.02.006

[28] Akgun, A.; Dag, S.;Bulut, F. Landslide susceptibility mapping for a landslide-prone area (Findikli, NE of Turkey) by likelihood-frequency ratio and weighted linear combination models. // Environmental Geology. 54, 6(2008), pp. 1127-1143. DOI: 10.1007/s00254-007-0882-8

[29] Chen, H.; Zeng, Z. Deformation prediction of landslide based on improved back-propagation neural network. // Cognitive Computation. 5, 1(2013), pp. 56-62. DOI:

10.1007/s12559-012-9148-1
[30] Lee, S.; Ryu, J. H.; Won, J. S.; Park, H. J. Determination and application of the weights for landslide susceptibility mapping using an artificial neural network. // Engineering Geology. 71, 3(2004), pp. 289-302. DOI: 10.1016/S0013-7952(03)00142-X
[31] Neaupane, K. M.; Achet, S. H. Use of backpropagation neural network for landslide monitoring: a case study in the higher Himalaya. // Engineering Geology. 74, 3(2004), pp. 213-226. DOI: 10.1016/j.enggeo.2004.03.010
[32] Fen, F. Volterra adaptive real-time prediction of multivariate chaotic time series. // Systems Engineering and Electronics. 10, (2009).
[33] Huang, F. M.; Tian, Y. G. WA-VOLTERRA coupling model based on chaos theory for monthly precipitation forecasting. // Earth Science. 39, 3(2014), pp. 368-374.
[34] Orsenigo, C.; Vercellis, C. Combining discrete SVM and fixed cardinality warping distances for multivariate time series classification. // Pattern Recognition. 43, 11(2010), pp. 3787-3794. DOI: 10.1016/j.patcog.2010.06.005
[35] Cao, L.; Tay, F. E. Financial forecasting using support vector machines. // Neural Computing & Applications. 10, 2(2001), pp. 184-192. DOI: 10.1007/s005210170010
[36] Amari, S. I.; Wu, S. Improving support vector machine classifiers by modifying kernel functions. // Neural Networks. 12, 6(1999), pp. 783-789. DOI: 10.1016/S0893-6080(99)00032-5
[37] Feng, X. T.; Zhao, H.; Li, S. Modeling non-linear displacement time series of geo-materials using evolutionary support vector machines. // International journal of rock mechanics and mining sciences. 41, 7(2004), pp. 1087-1107. DOI: 10.1016/j.ijrmms.2004.04.003
[38] Kavzoglu, T.; Sahin, E. K.; Colkesen, I. Landslide susceptibility mapping using GIS-based multi-criteria decision analysis, support vector machines, and logistic regression. // Landslides. 11, 3(2014), pp. 425-439. DOI: 10.1007/s10346-013-0391-7
[39] Lian, C.; Zeng, Z.; Yao, W. et al. Ensemble of extreme learning machine for landslide displacement prediction based on time series analysis. // Neural Computing and Applications. 24, 1(2014), pp. 99-107. DOI: 10.1007/s00521-013-1446-3
[40] Lian, C.; Zeng, Z.; Yao, W.; Tang, H. Displacement prediction model of landslide based on a modified ensemble empirical mode decomposition and extreme learning machine. // Naturalhazards. 66, 2(2013), pp. 759-771. DOI: 10.1007/s11069-012-0517-6
[41] Wang, X.; Han, M. Improved extreme learning machine for multivariate time series online sequential prediction. // Engineering Applications of Artificial Intelligence. 40, (2015), pp. 28-36. DOI: 10.1016/j.engappai.2014.12.013
[42] Handoko, S. D.; Keong, K. C.; Soon, O. Y. et al. Extreme learning machine for predicting HLA-peptide binding. // In Advances in Neural Networks-ISNN 2006, Springer Berlin Heidelberg. (2006), pp. 716-721. DOI: 10.1007/11760191_105
[43] Huang, G. B.; Zhu, Q. Y.; Siew, C. K. Extreme learning machine: theory and applications. // Neurocomputing.70, 1(2006), pp. 489-501. DOI: 10.1016/j.neucom.2005.12.126
[44] Sun, Z. L.; Choi, T. M.; Au, K. F.et al. Sales forecasting using extreme learning machine with applications in fashion retailing. // Decision Support Systems. 46, 1(2008), pp. 411-419. DOI: 10.1016/j.dss.2008.07.009
[45] Wang, X.; Han, M. Online sequential extreme learning machine with kernels for nonstationary time series prediction. // Neurocomputing. 145, (2014), pp. 90-97. DOI: 10.1016/j.neucom.2014.05.068
[46] Suresh, S.; Venkatesh, B. R.; Kim, H. J. No-reference image quality assessment using modified extreme learning machine classifier. // Applied Soft Computing. 9, 2(2009), pp. 541-552. DOI: 10.1016/j.asoc.2008.07.005
[47] Huang, G. B.; Ding, X.; Zhou, H. Optimization method based extreme learning machine for classification. // Neurocomputing. 74, 1 (2010), pp. 155-163. DOI: 10.1016/j.neucom.2010.02.019
[48] Rong, H. J.; Ong, Y. S.; Tan, A. H.; Zhu, Z. Afast pruned-extreme learning machine for classification problem. // Neurocomputing, 72, 1(2008), pp. 359-366. DOI: 10.1016/j.neucom.2008.01.005
[49]Mohammed, A. A.; Minhas, R.; Wu, Q. J.; Sid-Ahmed, M. A. Human face recognition based on multidimensional PCA and extreme learning machine. // Pattern Recognition. 44, 10(2011), pp. 2588-2597. DOI: 10.1016/j.patcog.2011.03.013
[50] Zong, W.; Huang, G. B. Face recognition based on extreme learning machine.// Neurocomputing. 74, 16(2011), pp. 2541-2551. DOI: 10.1016/j.neucom.2010.12.041
[51] Shen, G.; Xie, Z. Three Gorges Project: chance and challenge. // Science. 304, 5671(2004), pp. 681-681. DOI: 10.1126/science.304.5671.681b
[52] Yin, Y.; Wang, H.; Gao, Y.; Li, X. Real-time monitoring and early warning of landslides at relocated Wushan Town, the Three Gorges Reservoir, China. // Landslides. 7, 3(2010), pp. 339-349. DOI: 10.1007/s10346-010-0220-1
[53] Chen, D. Y.; Han, W. T. Prediction of Multivariate Chaotic Time Series via Radial Basis Function Neural Network. // Complexity. 18, 4(2013), pp. 55-66. DOI: 10.1002/cplx.21441
[54] Shang-qing, W.; Jin-jun, X.; Mian, L. Study of warning of dangerous state of Baishuihe Landslide in Three Gorges Reservoir Area. // Geomatics and Information Science of Wuhan University. 34, 10(2009), pp. 1218-1221.
[55] Aqil, M.; Kita, I.; Yano, A.; Nishiyama, A. Analysis and prediction of flow from local source in a river basin suing a Neuro-fuzzy modeling tool. // Journal of Environmental Management. 85, 1(2007), pp. 215-223. DOI: 10.1016/j.jenvman.2006.09.009
[56] Daliakopoulos, I. N.; Coulibaly, P.; Tsanis, I. K. Groundwater level forecasting using artificial neural networks. // Journal of Hydrology. 309, (2005), pp. 229-240. DOI: 10.1016/j.jhydrol.2004.12.001
[57] Wong, H.; Ip, W. C.; Zhang, R. Q.; Xia, J. Non-parametric time series models for hydrological forecasting. // Journal of Hydrology. 332, 3-4(2007), pp. 337-347. DOI: 10.1016/j.jhydrol.2006.07.013
[58] Liu, L. W.; Lin, Z. X.; Liu, L. M. Analysis of Bazimen Landslide Soil by Laser-Induced Breakdown Spectroscopy. // High Power Laser and Particle Beams. 23, 7(2011), pp. 1827-1830. DOI: 10.3788/HPLPB20112307.1827
[59] Ehret, D.; Rohn, J.; Schleier, M. Landslide reliability analysis based on transfer coefficient method: a case study from Three Gorges Reservoir. // Journal of Earth Science. 23, 2(2012), pp. 187-198. DOI: 10.1007/s12583-012-0244-7

**Authors' addresses**

***Fa-ming Huang, Ph.D.***
Geological Survey Institution of China University of Geosciences,
Lumo Road 388, Hongshan District,
Wuhan, 430074, Hubei, P. R. China
Phone: 15002776908
E-mail: huang1503518@sina.cn

***Kunlong Yin, Professor,*** *corresponding author*
Faculty of Engineering, China University of Geosciences,
Lumo Road 388, Hongshan District,
Wuhan, 430074, Hubei, P. R. China
Phone: 13871066785
E-mail: yinklong@163.com

***Tao He***
College of Oujiang of Wenzhou University,
325035, Wenzhou, P. R. China
E-mail: hetao1030@126.com

***Chao Zhou***
Faculty of Engineering, China University of Geosciences,
Lumo Road 388, Hongshan District,
Wuhan, 430074, Hubei, P. R. China

***Jun Zhang***
Faculty of Engineering, China University of Geosciences,
Lumo Road 388, Hongshan District,
Wuhan, 430074, Hubei, P. R. China